Correspondence to:
J. Friberg,
johan.friberg@nuclear.lu.se

Influence of volcanic eruptions on midlatitude upper tropospheric aerosol and consequences for cirrus clouds

Johan Friberg[1], Bengt G. Martinsson[1], Moa K. Sporre[1], Sandra M. Andersson[1], Carl A. M. Brenninkmeijer[2], Markus Hermann[3], Peter F. J. van Velthoven[4], and Andreas Zahn[5]

[1]Department of Physics, Lund University, Lund, Sweden, [2]Max Planck Institute for Chemistry, Mainz, Germany, [3]Leibniz Institute for Tropospheric Research, Leipzig, Germany, [4]Royal Netherlands Meteorological Institute, de Bilt, Netherlands, [5]Institute for Meteorology and Climate Research, Karlsruhe Institute of Technology, Karlsruhe, Germany

Abstract The influence of downwelling stratospheric sulfurous aerosol on the UT (upper troposphere) aerosol concentrations and on cirrus clouds is investigated using CARIBIC (Civil Aircraft for Regular Investigation of the Atmosphere Based on an Instrument Container observations) (between 1999–2002 and 2005–2013) and the cirrus reflectance product from Moderate Resolution Imaging Spectroradiometer (MODIS). The initial period, 1999–2002, was volcanically quiescent after which the sulfurous aerosol in the LMS (lowermost stratosphere) (S_{LMS}) became enhanced by several volcanic eruptions starting 2005. From 2005 to 2008 and in 2013, volcanic aerosol from several tropical eruptions increased S_{LMS}. Due to consequent subsidence, the sulfur loading of the upper troposphere (S_{UT}) was increased by a factor of 2.5 compared to background levels. Comparison of S_{LMS} and S_{UT} during the seasons March–July and August–November shows a close coupling of the UT and LMS. Finally, the relationship between S_{LMS} and the cirrus cloud reflectance (CR) retrieved from MODIS spectrometer (on board the satellites Terra and Aqua) is studied. S_{LMS} and CR show a strong anticorrelation, with a factor of 3.5 increase in S_{LMS} and decrease of CR by $8 \pm 2\%$ over the period 2001–2011. We propose that the increase of S_{LMS} due to volcanism has caused the coinciding cirrus CR decrease, which would be associated with a negative radiative forcing in the Northern Hemisphere midlatitudes.

1. Introduction

The present study focuses on particulate matter collected in the upper troposphere (UT) and lowermost stratosphere (LMS) by the passenger aircraft based CARIBIC (Civil Aircraft for Regular Investigation of the Atmosphere Based on an Instrument Container) observatory [*Brenninkmeijer et al.*, 2007]. The transport of air enriched in ozone and particulate sulfur from the stratosphere into the troposphere can be monitored by CARIBIC throughout the seasons and years. Although the cruise altitude is nearly constant, the variable altitude of the extratropical tropopause allows the retrieval of vertical profiles across the tropopause and a sampling both in the UT and in the LMS. By this, CARIBIC can follow the fate of stratospheric aerosol.

The sulfurous fraction is the major component of stratospheric aerosol [*Deshler*, 2008; *Rosen*, 1971]. Recent studies [*Martinsson et al.*, 2009; *Murphy et al.*, 1998; *Schmale et al.*, 2010] find that the aerosol also contains significant amounts of carbonaceous species. In addition, small crustal [*Andersson et al.*, 2013] and meteoric [*Murphy et al.*, 2014] components are found in stratospheric aerosol particles.

The two largest sources of sulfuric acid particles in the stratosphere are the photolysis/oxidation of OCS and SO_2 [*Crutzen*, 1976; *Weisenstein et al.*, 1997], with a minor contribution from direct injection of sulfurous particles from the tropical troposphere. SO_2 forms sulfuric acid at all altitudes in the stratosphere via oxidation by radicals, while OCS is photooxidized chiefly at higher altitudes in the stratosphere. Injections of particulate matter via volcanism are by far the source inducing most variability in the stratospheric aerosol [*Robock*, 2000]. Remote sensing at lidar stations (in Boulder, Colorado, and in Mauna Loa, Hawaii) revealed a trend of increasing aerosol burden in the stratosphere (20–25 km altitude) in the period 2000–2009 [*Hofmann et al.*, 2009], which was later shown to be caused by volcanism in the tropics [*Vernier et al.*, 2011]. The stratosphere's increasing aerosol concentration has been found to cause a negative radiative forcing of $-0.1\,Wm^{-2}$ [*Solomon et al.*, 2011]. Later studies

[*Andersson et al.*, 2015; *Ridley et al.*, 2014] find that also volcanic aerosol in the LMS contributes significantly to the climate forcing in that period. These findings indicate that volcanism is a major cause for the deviations between the actual and predicted [*Flato et al.*, 2013] global warming since year 2000.

The Brewer-Dobson circulation transports air from the tropical tropopause via the middle and upper stratosphere (deep branch) and quasi-horizontally (shallow branch) to midlatitude and high latitude [*Holton et al.*, 1995]. The deep branch brings air with high concentrations of O_3 and sulfuric acid particles from the Junge layer to lower altitudes where it mixes with air from the lower branch. Whereas the deep branch transports air to midlatitudes within years, the shortcut via the lower branch requires only a few months.

The LMS is restricted downward by the tropopause, while its upper boarder is defined as the 380 K isentrope [*Holton et al.*, 1995]. Stratospheric air with high concentrations of O_3 and particulate sulfur that reaches the LMS undergoes mixing with air from the troposphere. On a local scale, mixing through the tropopause results in a 2–3 km thick layer with strong vertical gradients of trace gases [*Hoor et al.*, 2004; *Pan et al.*, 2004], called the extratropical tropopause transition layer. Seasonality in the strength of the transport paths results in seasonally varying proportions of stratospheric and tropospheric air in the LMS leading to, for example, varying ozone concentrations during the year, with the highest concentrations in spring and lowest during fall [*Zahn and Brenninkmeijer*, 2003]. Via observations of trace gas concentrations, *Bönisch et al.* [2009] revealed a seasonal cycle in the mean age of air in the LMS, decreasing from spring to fall.

Mixing through the tropopause eventually leads to transport of sulfur-rich stratospheric aerosol to the midlatitude UT, where particulate sulfur concentrations are substantially lower compared to the LMS [*Martinsson et al.*, 2005]. Sulfur compounds can also be transported from the surface by deep convection and warm conveyor belts and then lead to particle formation in the UT. *Guan et al.* [2010] report that large forest fires contributed to about 10 occurrences of pyroconvection, in 2006–2009, that could have transported biomass burning smoke to UT altitudes. Particles from this source type contain mostly carbonaceous matter with traces of metals such as potassium [*Reid et al.*, 2005]. However, *Murphy et al.* [2006] found that UT particles generally contain mixtures of sulfurous and carbonaceous components. Most of them contained no potassium, suggesting pyroconvection to be only a minor source of UT aerosol. Investigating particle morphologies, *Nguyen et al.* [2008] established that the sulfurous and carbonaceous components are internally mixed residing in different parts of the particles.

Aerosol particles in the UT are involved in the formation of cirrus clouds. Cirrus ice crystals either form homogeneously via freezing of supercooled solution droplets or heterogeneously when water crystallizes directly on ice nuclei (IN) [*Pruppacher and Klett*, 1997]. Mineral dust and metallic particles have been proposed to be the main suppliers of IN in the UT [*Cziczo et al.*, 2013; *DeMott et al.*, 2003]. Soot particles may also act as IN but at lower temperatures than mineral dust [*Hoose and Möhler*, 2012]. Recent measurements indicate that soot IN concentrations from aircraft have been underestimated [*Schumann et al.*, 2013], and the question whether soot particles from aviation affect cirrus properties has been the focus of several modeling studies recently. *Gettelman and Chen* [2013] found no effect on cirrus from aviation soot while *Zhou and Penner* [2014] found the soot to significantly alter the cirrus cloud properties. The different outcomes of the studies are caused by the different assumptions regarding the nucleation efficiency of soot. Besides soot, jet engines emit metallic elements [*Agrawal et al.*, 2008] that might add somewhat to the concentration of IN in the UT. Coating of IN, by compounds such as sulfuric acid, has in laboratory experiments been found to decrease aerosol particle effectiveness to act as IN [*Hoose and Möhler*, 2012].

Homogeneous nucleation was for many years considered to be the dominant formation mechanism for cirrus clouds [*Jensen et al.*, 2010], and in situ measurements of temperature, relative humidity, ice water content, particle size, and fall velocities have been found to confirm this [*Mitchell et al.*, 2011]. However, a recent study, investigating ice particle residuals [*Cziczo et al.*, 2013], indicates that heterogeneous freezing is the dominant mechanism for cirrus clouds over Central America and parts of North America. Heterogeneous ice nucleation has recently been incorporated in model studies of cirrus clouds [*Barahona et al.*, 2014; *Kuebbeler et al.*, 2014; *Storelvmo and Herger*, 2014]. One such study, *Barahona et al.* [2014], finds homogeneous freezing to be the dominant mechanism globally except over central Asia, the Arctic, and the west coast of North America. However, *Zhou and Penner* [2014] find that if aircraft soot emissions

provide additional IN, they could shift the freezing regime from homogeneous to heterogeneous freezing over North America, Europe, and the North Atlantic Ocean.

Whether or not volcanic aerosols injected into the stratosphere can affect cirrus clouds in the UT has been the topic of several research papers and the conclusions differ. One satellite study found an increase in high-level cloudiness after the El Chichon and Mount Pinatubo eruptions [*Song et al.*, 1996], while other satellite studies found no changes in cirrus properties after the Mount Pinatubo eruption [*Luo et al.*, 2002; *Wylie and Menzel*, 1999]. Moreover, modeling studies of the same event using only homogeneous nucleation theory find increased ice crystal number concentrations in cirrus clouds after the eruption [*Karcher and Lohmann*, 2002; *Lohmann et al.*, 2003]. Recently, a satellite study by *Campbell et al.* [2012] found cirrus clouds formed by seeding from a stratospheric layer of volcanic aerosol from the Kasatochi eruption in 2008.

Cirrus clouds are estimated to have an overall larger impact on the long-wave than on the short-wave radiation, resulting in a net warming of the surface [*Boucher et al.*, 2013; *Chen et al.*, 2000]. Estimations of radiative forcing from cirrus clouds hold considerable uncertainties [*Boucher et al.*, 2013] depending on a range of factors [*Baran*, 2009] including ice crystal shape, size, number concentration, cloud coverage, cloud thickness, and temperature [*Fusina et al.*, 2007].

In recent studies we investigated variations in the LMS aerosol concentrations during periods of tropical [*Friberg et al.*, 2014] and extratropical [*Andersson et al.*, 2013; *Martinsson et al.*, 2009] volcanism. We now investigate the influence on midlatitude UT aerosol concentrations of volcanic aerosol from the LMS, based on elemental analyses of aerosol samples collected by CARIBIC between 1999 and 2013. Perturbation of LMS aerosol by volcanism during these 15 years ranged from low to moderate. With the direct impact of volcanic aerosol in the UT/LMS having been addressed by *Andersson et al.* [2015], we now present a comparison between measured UT/LMS aerosol concentrations and MODIS (Moderate Resolution Imaging Spectroradiometer) retrieved cirrus reflectance (CR), in the light of the indirect climate impact of volcanism.

2. Methods

The period 1999–2013 was covered by CARIBIC in a near monthly rhythm, except for the 2.5 year period mid-2002 to 2005, which was used for a transition from CARIBIC 1 (Boeing 767 ER aircraft, leaving Düsseldorf and Munich airports) [*Brenninkmeijer et al.*, 1999] to CARIBIC 2 (Airbus A340-600 aircraft based in Frankfurt) [*Brenninkmeijer et al.*, 2007]. The CARIBIC system is currently based on a 1.5 t automated measurement container constituting a compact laboratory. The container is installed monthly for 2–6 consecutive flights in a Lufthansa passenger Airbus A340-600, which has been retrofitted for this task with a permanent inlet system having inlet probes for water vapor, cloud water, aerosol, and trace gases. So far about 100 publications deal with methods and results (www.caribic-atmospheric.com). The CARIBIC system is part of IAGOS (In situ Aircraft for a Global Observing System, www.iagos.org)

2.1. Air-Inlet for Aerosol Sampling

Different inlet systems were used for CARIBIC phases #1 and #2. The inlet used in phase #1 had an estimated sampling efficiency of 90% for 0.1–1 μm particles [*Hermann et al.*, 2001]. The presently used system (phase #2) has a sampling efficiency of 60% for 5 μm particles and a high transmission (>90%) for submicron particles [*Martinsson et al.*, 2014; *Rauthe-Schöch et al.*, 2012]. A cyclone with close to 100% transmission for submicron particles [*Nguyen et al.*, 2006] and a cutoff size of 2 μm are installed to reduce the influence from larger particles.

2.2. The Aerosol Sampler

Aerosol particles with aerodynamic diameters of 0.08–2 μm were collected using an automated aerosol sampler with close to 100% collection efficiency [*Nguyen et al.*, 2006] based on the use of impactors. Particles were deposited on 0.2 μm thin AP1™ polyimide films [*Papaspiropoulos et al.*, 1999]. Similar impactors were used during phases #1 and #2. The phase #2 (phase #1) device consists of 14 (12) channels for sequential samples. In addition, 2 channels were used to collect integral samples, to check for contaminations. Typical air volumes of 0.25 (0.09) m^3 STP (standard temperature and pressure) were sampled during 100 (150) min or 1500 (2200) km flight distance. Sampling is suspended when the pressure exceeds 350 hPa (landing and takeoff cycles) to avoid sampling of aerosol from lower altitudes.

2.3. Aerosol Composition Analysis

Chemical characterization of aerosol particles was obtained using PIXE (particle-induced X-ray emission) [*Johansson and Campbell*, 1988]. Samples were irradiated by a proton beam of 2.55 MeV at the Lund ion beam analysis facility. Elemental concentrations were derived for elements with atomic numbers larger than 15, with an estimated accuracy of 10% [*Martinsson et al.*, 2014; *Papaspiropoulos et al.*, 1999]. Here we focus on the sulfur data, which have a typical minimum detection limit (MDL; detection of an element with a confidence of 99%) of 2 ng m^{-3} STP. Sulfur concentrations below MDL were set to MDL/2. Detection frequencies for sulfur were 99% (UT) and 100% (LMS).

2.4. Sampling in the Midlatitude UT/LMS

Because the CARIBIC aircraft collects samples in a narrow altitude interval (9–12 km above sea level), either the extratropical UT/LMS or the tropical middle troposphere is investigated. However, due to the movement of the tropopause level relative to the aircraft flight track, air masses with vertical distances relative to the tropopause from 5 km below the tropopause to 5 km above the tropopause are probed [*Zahn et al.*, 2014]. At midlatitude and high latitude the tropopause is frequently crossed. In the present study, samples collected on latitudes south of 30°N were excluded to keep the influence from tropical air low.

2.4.1. The Dynamical Tropopause

We used potential vorticity (PV) to define the tropopause. PV values were derived from archived ECMWF (European Centre for Medium-range Weather Forecast) analyses with a resolution of 1° × 1° in the horizontal at 91 vertical hybrid sigma-pressure model levels. PV values were interpolated linearly in latitude, longitude, log pressure, and time to the location of the aircraft and for each sample averaged over the duration of sampling. Generally, PV values of 1.5–3.5 potential vorticity unit (PVU) [*Hoerling et al.*, 1991; *Hoinka*, 1997] are employed for defining the dynamical tropopause. Here we use 2 PVU.

2.4.2. Classification of UT and LMS Samples

Samples with an average PV > 2 PVU were classified to be stratospheric, while UT samples were those below 1.5 PVU. The sampling time for the impactor is relatively long, sometimes resulting in samples representing air from both the UT and the LMS. To eliminate a bias in the UT aerosol concentration from samples partially taken in the LMS, samples collected at average PV lower than 1.5 PVU were excluded from this investigation, if the aircraft had crossed the tropopause (2 PVU) during the sampling interval.

2.5. Exclusion of Samples Affected by Fresh Volcanic Aerosol

Volcanic clouds reaching the UT/LMS can enhance the background aerosol concentrations tremendously. In the weeks following an eruption the emitted SO$_2$ is converted to sulfate and the resulting volcanic aerosol mixes at various degrees with the background. Moreover, fresh volcanic aerosol injected in the UT is susceptible to scavenging by precipitation formation. Therefore, samples collected within 30 days after volcanic eruptions that reached the extratropical UT/LMS (listed in Table 1) were excluded to prevent bias from patchiness in aerosol concentrations and influence from large ash particles. An extremely high particulate sulfur concentration was observed for one additional sample (August 2001). Trajectory analysis shows direct transport from the area of an eruption of Bezymianny, at the Kamchatka peninsula, Russia. Hence, this sample happened to have been collected in a fresh volcanic cloud was also excluded.

2.6. Contour Graphs

The geographical distribution of particulate sulfur concentration is illustrated by using a contour graph. It was produced by splitting each sample into 10 equidistant parts along the flight track, and the average position of the aircraft in longitude × latitude was calculated for each part, yielding 10 sample parts of typically 150 km along the flight route. These parts were assigned aerosol concentrations according to the analytical results and were sorted into and averaged on a longitude × latitude grid of 5° × 5°, and a center-weighted 2-D smoothing was performed. Grid cells with fewer than 10 samples in their eight nearest surrounding grid cells were excluded to reduce the impact from regions where few observations were made. The data were then 2-D interpolated to 1° × 1° (longitude × latitude) to form the presented graph. A similar contour graph was created illustrating the geographical variation of potential vorticity.

Table 1. Volcanic Eruptions in the Tropics and in the Northern Extratropics, Identified to Have Influenced the Particulate Sulfur Concentrations in the LMS (Also Marked in Figure 3) in the Period 1999–2013

Eruption Date[a]	Volcano	SO_2 (Tg)	VEI[a]	Longitude[a]	Latitude[a]
01-27-2005	Manam	0.09[b]	4	145	−4.1
05-20-2006	Soufriere Hills	0.2[c]	3	−62	16.7
10-07-2006	Rabaul	0.2[d]	4	152	−4.3
07-12-2008	Okmok	0.1[e]	4	−168	55.3
08-07-2008	Kasatochi	2[f]	4	−176	52.2
03-20-2009	Redoubt	0.08[g]	3	−153	60.5
06-12-2009	Sarychev	1.2[h]	4	153	48.1
05-21-2011	Grimsvötn	0.4[i]	4	−17.3	64.4
06-12-2011	Nabro	1.5[i]	4	41.7	13.4

[a]Volcanic explosivity index, from *Global Volcanism Program* [2011].
[b]*Prata and Bernardo* [2007].
[c]*Carn and Prata* [2010].
[d]*Carn et al.* [2009].
[e]*Thomas et al.* [2011].
[f]*Yang et al.* [2010].
[g]*Lopez et al.* [2009].
[h]*Haywood et al.* [2010].
[i]*Clarisse et al.* [2012].

2.7. Satellite Measurements

We use satellite data of cirrus clouds from the MODIS instruments. One MODIS instrument is placed on the satellite Terra, launched in December 1999, and the other on Aqua, launched in May 2003. Terra has a descending orbit while Aqua has an ascending orbit and their equatorial crossing times are 10:30 and 13:30 local solar time [*Platnick et al.*, 2003]. MODIS is a whiskbroom scanning radiometer with 36 wavelength channels spread between 0.620 and 14.4 μm. One of these channels, centered at 1.38 μm, was selected specifically for the study of cirrus clouds [*Gao and Kaufman*, 1995]. Incoming solar radiation at 1.38 μm is either reflected and scattered by the cirrus clouds or completely absorbed by the underlying atmosphere due to high water vapor absorption at this wavelength [*Gao et al.*, 2002; *Meyer and Platnick*, 2010]. However, 1–10% of the atmospheric water vapor is normally located above the cirrus clouds which results in attenuation of the 1.38 μm signal. To quantify this attenuation, a scaling factor is calculated from the slope of scatterplots of the reflectance in the 1.38 μm channel versus the reflectance from a cannel in the visible spectrum (0.66 μm) [*Gao et al.*, 2002]. Each MODIS granule (2030 × 1354 pixels) is divided into 16 subgranules, and a scaling factor is calculated for each of these subgranules. The scaling factors are then interpolated to avoid a chessboard effect, and the reflectance from the cirrus clouds for each pixel is calculated [*Gao et al.*, 2002; *Meyer and Platnick*, 2010]. Our analysis is based on the Level 3 monthly averaged CR with a resolution of 1° × 1°.

During dry atmospheric conditions not all solar radiation at 1.38 μm will be absorbed by the underlying atmosphere. Hence, reflection from the surface or lower lying clouds can contaminate the CR product [*Meyer and Platnick*, 2010]. The atmospheric water vapor product from MODIS has therefore been used to screen out dry atmospheric conditions. Similar results were obtained when using the total column water vapor from the ECMWF. The limit was set to 0.4 cm after recommendation from B.-C. Gao (personal communication, 2014) and investigation of the CR and atmospheric water vapor data. Since the same area is to be used for all monthly averages, pixels that have atmospheric water vapor less than 0.4 cm during the investigated years are removed from the entire data set. This was done for Terra and Aqua separately, but the areas included are very similar, see Figure 1. It is mainly continental areas over central North America and Asia, in particular ranges of high mountains, that are excluded but also some small ocean areas east of these continents. In order to compare the MODIS-retrieved CR against the CARIBIC measurements, only data from 30°N to 60°N are used to form average monthly cirrus products. Due to the latitude dependence of temperature and therefore atmospheric water vapor concentration, the fraction of pixels that are too dry increases with latitude. To avoid bias from this phenomenon, zonal averages were computed using 1° × 1° pixels. These averages were then weighted according to area in order to obtain the average CR for 30–60°N. An estimation of the uncertainty in the averages was calculated using error propagation on the standard deviation of the daily mean of each 1° × 1° pixel. Internal checkups of the MODIS instrument on Terra were carried out
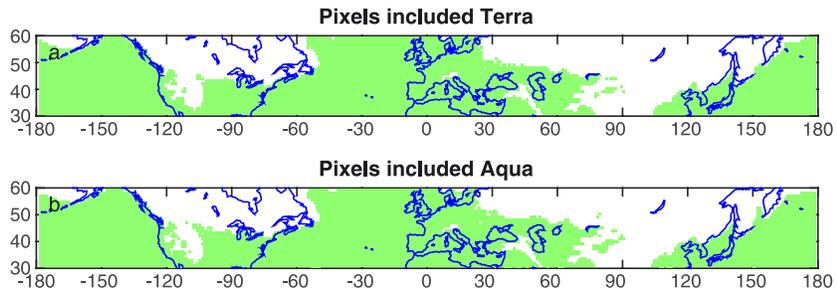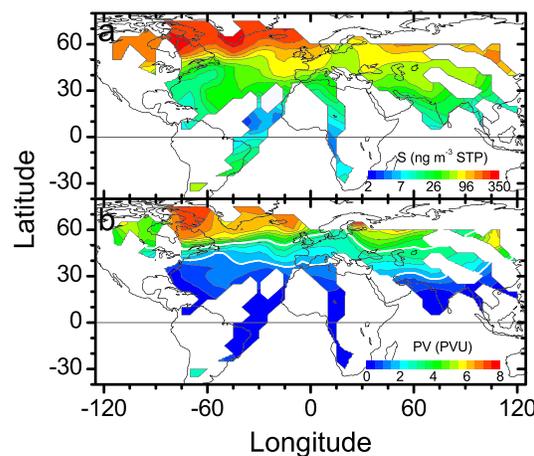
Figure 1. Illustration of the geographical areas included in the calculations of the MODIS cirrus reflectance for (a) Terra and (b) Aqua.

during spring and summer year 2000. The data from this period were not used. The averaged Aqua CR values are somewhat higher (13–19%) than the Terra values. This could be caused by the later overpass time of Aqua which enables more convective activity and thereby larger contribution from cirrus anvils to the CR.

3. Results

3.1. Geographical Distributions of Sulfur and PV

CARIBIC measurements over the years cover latitudes 30°S to 70°N and longitudes 120°W to 120°E. Figure 2a provides a geographical view of the particulate sulfur concentrations at 9-12 km altitude for all samples, tropospheric and stratospheric. The concentration clearly depends on the geographical location of sampling. A strong latitudinal gradient of the concentration of particulate sulfur is observed, with higher concentration in the North Hemisphere (NH) midlatitudes, than in the subtropics. *Martinsson et al.* [2005] found a correlation of sulfur and PV in the LMS, due to downwelling of particulate sulfur from the higher altitudes. A comparison of the geographical distribution of particulate sulfur concentrations (Figure 2a) and that of the average PV during sampling (Figure 2b) indicates the possible stratospheric origin of high sulfur concentrations. Downwelling of sulfur-rich stratospheric air can strongly enhance the particulate sulfur mass concentrations in the midlatitudes tropopause region. The samples in the subtropics are somewhat influenced by stratospheric air, while the tropical samples are purely tropospheric. The gradient to the tropics could also be caused by other differences in source patterns as well as by more efficient wet scavenging of the hygroscopic sulfur particles in the tropics by deep convective clouds. The following sections deal with the coupling of the LMS and midlatitude UT.


Figure 2. Contour graphs illustrating the geographical distribution of (a) particulate sulfur concentrations and (b) PV, based on all aerosol samples collected by CARIBIC in the period 1999–2013. The white lines in Figure 2b mark the PV isopleths of 1.5 and 3.5 PVU, the range in PV where the dynamical tropopause normally is set.

3.2. Volcanic Influence on Particulate Sulfur in the Midlatitude UT

Over the 15 year time span considered, particulate sulfur concentrations in the UT and LMS vary by a factor of about 100 (Figure 3). In parts of this period the LMS serves as a reservoir of volcanic aerosol that eventually is transported to the midlatitude UT. To investigate a coupling between the UT and LMS we will group data depending on the magnitude of volcanic influence on the aerosol concentrations. In the LMS, the sulfur concentrations need to be normalized by PV in order to compensate for the strong gradient of sulfur in the LMS and to highlight deviations from the nonvolcanically influenced particulate sulfur distribution. UT data are scarce as most of the midlatitude
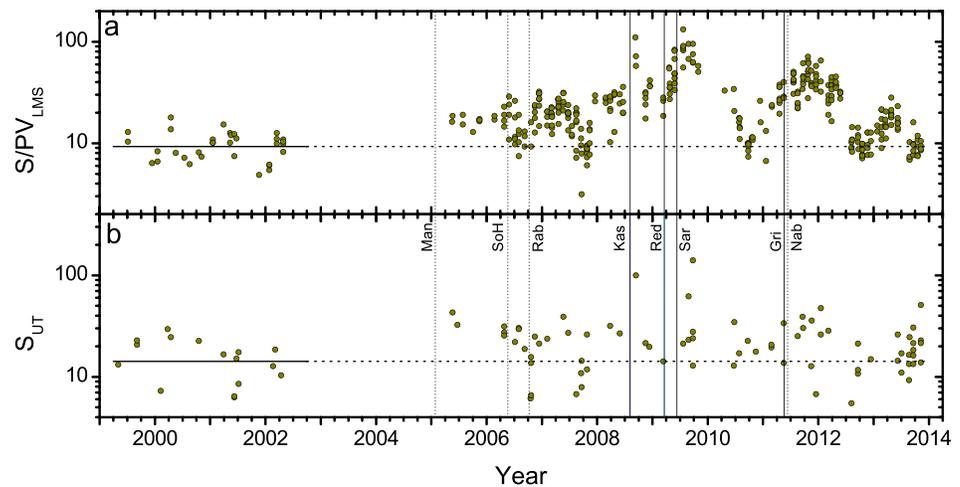
Figure 3. Temporal variations in the northern midlatitude of (a) S/PV values in the LMS (S/PV$_{LMS}$; ng m^{-3} STP/PVU) and (b) sulfur concentrations in the UT (S$_{UT}$; ng m^{-3} STP). The horizontal lines show the geometric averages for the period 1999–2002. The vertical lines mark the volcanic eruptions identified to have influenced the particulate sulfur concentrations in the LMS. The vertical dashed and full lines represent the eruptions in the tropics and northern midlatitudes, respectively. Data for the 30 days following these eruptions are excluded, also in the following figures.

samples were collected in the LMS. Thus, details in the variability in sulfur concentrations do not show as clearly in the UT as in the LMS. We will therefore use the LMS sulfur concentrations as a more distinct measure of the magnitude of the volcanic influence in the UT/LMS and divide the data into groups depending on the volcanic influence.
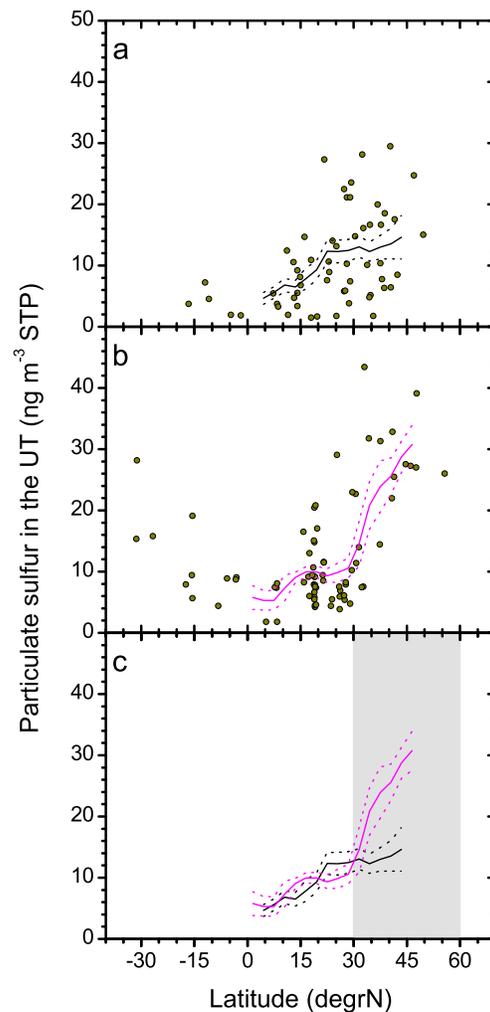
3.3. Grouping Data Depending on Volcanic Influence

The average S/PV ratio for the period 1999–2002 was low (Figure 3), indicating a time of low volcanic impact on the stratosphere [*Martinsson et al.*, 2005]. However, particulate sulfur was affected by volcanic aerosol to various degrees after the year 2005. The 3 year period mid-2002 to mid-2005 was not monitored by CARIBIC but is known to have had little volcanic activity [*Myhre et al.*, 2013].

In the period May 2005 to July 2008 the LMS aerosol was influenced by three volcanic eruptions in the tropics (Manam, Soufriere Hills, and Rabaul). They injected large amounts of SO$_2$ (Table 1) into the tropical stratosphere [*Vernier et al.*, 2011] that was subsequently, while being oxidized, transported to midlatitudes within the Brewer-Dobson (BD) circulation. Subsequent downwelling [*Friberg et al.*, 2014] explains the observed increase in the LMS sulfur concentrations from the 1999–2002 baseline. A concomitant increase in UT sulfur concentrations is evident (Figure 3).

Figure 3 shows several large peaks in S/PV, starting with the Kasatochi explosion in 2008, which eventually decline [*Martinsson et al.*, 2009] by transport across the tropopause into the UT. Extratropical volcanism then caused peaks of varying magnitudes in 2009–2010 [*Andersson et al.*, 2013] and in spring 2011, followed by an eruption of the tropical volcano Nabro. Nabro emitted about the same amount of SO$_2$ (1.5 Tg) as Kasatochi and Sarychev did (Table 1). After transport from the tropics to midlatitudes, downwelling through the LMS explains the observed rise in S/PV from late summer 2011. Volcanic clouds reaching the tropical stratosphere can affect the extratropical LMS for years via transport in the deep BD branch. However, the long-lasting perturbations after Nabro were limited to the first half of the year 2012, because most of the transport took place in the tropical transition layer or in the lower BD branch [*Bourassa et al.*, 2012]. Finally, remaining aerosol particles from the Nabro explosion transported in the deep BD branch slightly elevated the concentration level in spring/summer 2013.

Next, the data are divided into the following groups: (1) background conditions, (2) samples affected by direct injections into the LMS, and (3) samples influenced by volcanic aerosol downwelling from the stratosphere from above the 380 K isentrope. Thus, we derive the following:

1. The years 1999–2002 as the period that represents background levels.

2. Midlatitude eruptions penetrating the extratropical tropopause can cause a large impact on the LMS that lasts for months depending on their penetration depths. The combined injections from Kasatochi, Redoubt, and Sarychev caused such perturbations in the period August 2008 to December 2009.

3. When volcanic clouds have reached the tropical stratosphere the aerosol can induce long-term impact on the LMS aerosol concentration by transport to midlatitudes in the deep BD branch. Over the 15 years studied here, such perturbations occurred during several periods, with largely varying magnitudes. These periods are split in two categories based on the volcanic eruptions effect on the sulfur concentrations in the LMS, because averaging large concentration differences would complicate the forthcoming analyses. Category 3a represents periods strongly affected by volcanism (i.e., the period after Nabro's eruption, late summer 2011 to summer 2012), while category 3b combines an intermediately affected LMS (i.e., the periods May 2005 to July 2008 (until the Kasatochi eruption) and the year 2013).

In spite of the scarcity of UT data there are similarities in its variability in sulfur concentrations to that of the S/PV in the LMS. Peaks and periods of high S/PV in the LMS are reflected to some degree in the UT (Figure 3). For example, the peaks after the eruptions of Kasatochi and Sarychev, the decreasing concentrations from spring/summer to fall in 2006 and 2007, and the increased sulfur concentrations after the eruption of Nabro. These similarities indicate that the aerosol concentrations in the UT can be affected strongly by the LMS.

3.4. Impact on UT/LMS Aerosol From Tropical Volcanism

To explore the influence from tropical volcanism on the aerosol concentrations in the midlatitude UT we compare sulfur concentrations from the periods May 2005 to July 2008 and 2013 (Category 3b) to that of the period 1999–2002 (Category 1) (hereinafter termed periods 05-08/13 and 99–02, respectively).

Figure 4. The latitudinal variation of particulate sulfur in the UT during (a) March–July 99–02 and (b) March–July 05–08/13 (c) a direct comparison of the averaged profiles shown as lines in Figures 4a and 4b. The dashed lines illustrate the 95% confidence interval. The grey shaded area in Figure 4c marks the northern midlatitudes, the latitude band of interest in the following figures and discussions.

The LMS contains a larger proportion of midstratospheric air in spring and summer, compared to fall when a large fraction of the LMS' air is of recent tropospheric origin [*Bönisch et al.*, 2009]. Hence, in the period 05-08/13 elevated aerosol concentrations are expected in the LMS and midlatitude UT during spring when volcanic aerosol is brought down from higher altitudes, while concentrations in fall are expected to be more connected to the aerosol concentrations in the troposphere. We explore seasonal differences by combining data from the two periods into one season of large stratospheric influence (March–July) and one season with large tropospheric influence (September–November).

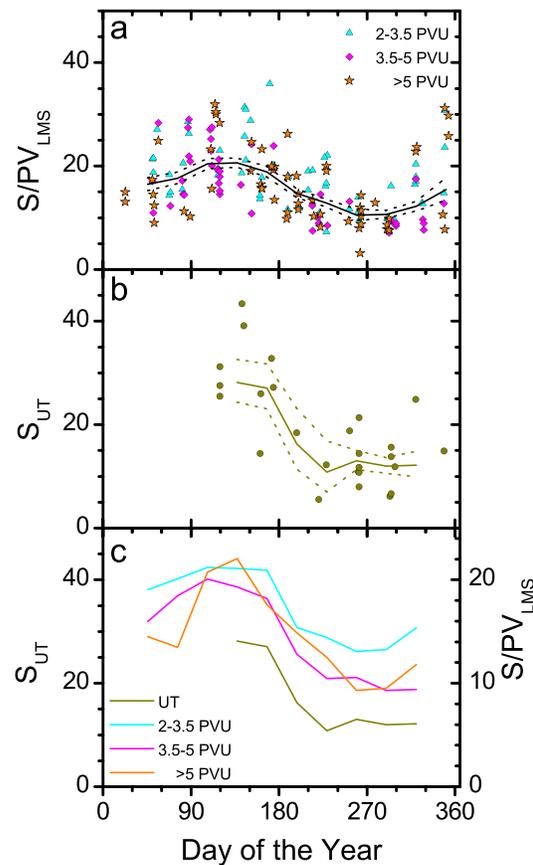### 3.4.1. Latitude Dependence of Particulate Sulfur UT Concentration

The latitudinal distribution of UT sulfur is displayed in Figure 4, revealing a clear tendency of increasing concentrations from the tropics to higher latitudes. For March–July, this gradient is more pronounced in the periods 05-08/13 than during 99–02 (Figures 4a and 4b). A direct comparison of the March–July moving averages (Figure 4c) shows similar concentration levels in the tropics and part of the subtropics.

Figure 5. Illustration of the seasonal variation of (a) S/PV at different PV intervals in the LMS (S/PV$_{LMS}$; ng m^{-3} STP/PVU), (b) the particulate sulfur concentration in the UT (S$_{UT}$; ng m^{-3} STP), and (c) a direct comparison of the S/PV$_{LMS}$ to the S$_{UT}$. The full and dashed lines illustrate the moving geometric averages with 95% confidence interval.

While the 05-08/13 periods show a steep increase with latitude, north of 30°N, the increase observed for the period 99–02 is not significant. This difference is largest at 45°N, which is the northernmost latitude for the average of 99–02, where the sulfur concentrations of 05-08/13 are twice that of 99–02. Hence, aerosol from tropical volcanic eruptions is detectable not only in the stratosphere but also in the midlatitude UT.

3.4.2. Seasonal Variation in the Midlatitude UT and LMS

The 05-08/13 data will now be further investigated in order to explore the origin of the particulate sulfur in the midlatitude UT and the cause of its seasonally varying concentrations. In Figure 5, the seasonally varying concentrations in the midlatitude UT are compared to the S/PV of different depths (PV levels) into the LMS.

In the LMS, high S/PV is observed in spring (Figure 5a) [Friberg et al., 2014] with a reduction during summer that reaches a minimum around August–October. The maximum coincides with the downwelling of stratospheric air from the deep BD branch carrying particulate sulfur to the LMS. The minimum in August–October again illustrates the small contribution from the deep BD branch in the LMS during late summer and fall.

We observe large similarities in the variation of sulfur in the UT to that in the LMS with the maximum concentrations found in May. In Figure 5c, a comparison of the moving averages for the sulfur concentrations in the UT and that of the S/PV in the LMS shows that the seasonal variations span approximately a factor of 2. In fall, the S/PV values close to the tropopause are higher than at higher PV values. However, this is not caused by higher sulfur concentrations at the lower PV values. Instead, it is an effect of a very weak dependence on PV of the sulfur concentrations in the LMS during fall [Friberg et al., 2014], resulting in high S/PV for low PV values.

4. Discussion

The strong similarities in the seasonally varying sulfur concentrations in the LMS and in the UT (Figure 5) indicate a high degree of coupling of their aerosol concentrations. Combined with previous findings of perturbations of the LMS from tropical volcanic injections transported to the LMS, these findings point to a strong influence from volcanism on the UT particulate sulfur concentration during the years 05-08/13.

To further investigate the impact of volcanism and the coupling of the UT and LMS we will extend the study with a direct comparison of the sulfur concentrations in the UT with the S/PV values in the LMS.

4.1. Transport of Volcanic Aerosol From the LMS to the UT
4.1.1. Volcanic Impact in Spring/Summer

To compare LMS and UT concentrations directly one needs to account for the variability in the transport across the extratropical tropopause. We therefore use the March–July data for a comparison in the season of large stratospheric influence. To deal with the scarcity of observations in the UT we group the years together, based on each year's average S/PV in the LMS, thus improving statistics. The years 2009 and 2011 are excluded in this comparison as midlatitude eruptions that reached the UT/LMS (Redoubt,
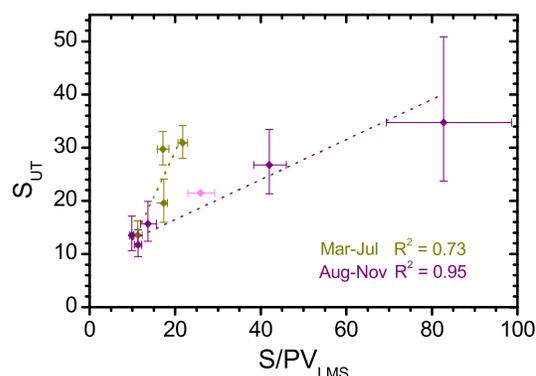
Figure 6. Comparison of the geometric averages of the particulate sulfur concentrations in the UT (S_{UT}; ng m^{-3} STP) to the S/PV in the LMS (S/PV$_{LMS}$; ng m^{-3} STP/PVU), for the seasons March–July (dark yellow diamonds) and August–November (magenta diamonds), for samples taken at PVs below 5 PVU. The dashed lines represent the linear regressions for the respective season. The error bars represents the geometric standard errors. The years that have been averaged for the season March–July, in order of their S/PV$_{LMS}$, are 2000–2002, 2010/2013, 2005/2006, and 2007/2008, while the August–November are 2007, 2010/2012, 2006, 2011 (Nabro), and 2009 (Sarychev). The 2008 (Kasatochi) data (light magenta, diamond) were excluded in the regression due to its poor statistics.

Sarychev, and Grimsvötn) occurred during the spring/summer. The year 2012 is excluded since only one UT observation is available. This results in four groups of years for comparison of the LMS and UT (2000–2002, 2010/2013, 2005/2006, and 2007/2008). The average sulfur concentrations in the UT and average S/PV in the LMS are compared in Figure 6 (dark yellow data points). Samples taken in air masses with PV values of less than 5 PVU are used here as they are expected to be more connected to the sulfur concentrations in the UT than those taken farther away from the tropopause [*Bönisch et al.*, 2009]. A positive correlation ($R^2 = 0.73$), with a significance level of 85%, emerges with a factor of 2.5 increase in the UT concentrations, ranging from 13 ng m^{-3} STP in the years 2000–2002 to 32 ng m^{-3} STP in 2007/2008. This correlation further indicates that downwelling from the stratosphere affects the aerosol concentration in the UT.

4.1.2. Volcanic Impact in Fall
For data taken in the fall, we have the possibility to extend the UT/LMS comparison to include the years that were affected by direct injections to the LMS by extratropical volcanism. To gain better statistics we extend the fall season to include August.

Aerosol samples collected in the August–November months after Kasatochi (August 2008), Sarychev (June 2009), and Nabro (June 2011) were all largely affected by volcanism. As Kasatochi exploded in August, samples from August and September 2008 are excluded.

The coupling between the LMS and UT is further explored via a comparison of the fall data (Figure 6, magenta data points) for the years when the LMS was strongly affected by volcanism (2008, 2009, and 2011) to that of the less affected years (2006, 2007, and 2012). Unfortunately, comparison to the period 99–02 is not possible, as only two observations of the sulfur concentrations in the LMS in fall are available. A linear regression of the fall data, results in a strong correlation ($R^2 = 0.95$) of high significance (>99%). The 2008 (Kasatochi) data are omitted in this calculation as only one observation from the UT is available. The strong correlation in fall, combined with the correlation found during spring/summer (see section 4.1.1), indicates that downwelling from the stratosphere strongly affects the particulate sulfur concentration in the UT. Interestingly, the slope in spring/summer is a factor 4 larger than in fall. The higher slope is attributed to increased stratosphere-to-troposphere transport [*Sprenger and Wernli*, 2003], resulting in a stronger influence from stratospheric aerosol in the UT.

4.2. Implications of Volcanic Impact on the UT
Whereas stratospheric aerosol affects Earth's radiation budget directly, tropospheric aerosol can affect the budget also indirectly, namely, by altering the occurrence and properties of clouds. In the previous sections the variability of sulfur in the northern midlatitude UT was found to be caused (i) by the seasonally varying subsidence of high-stratospheric air and (ii) by the varying contribution of volcanic aerosol mixed-in from the LMS. Next we will investigate whether volcanism influences the radiation budget via interaction with cirrus clouds.
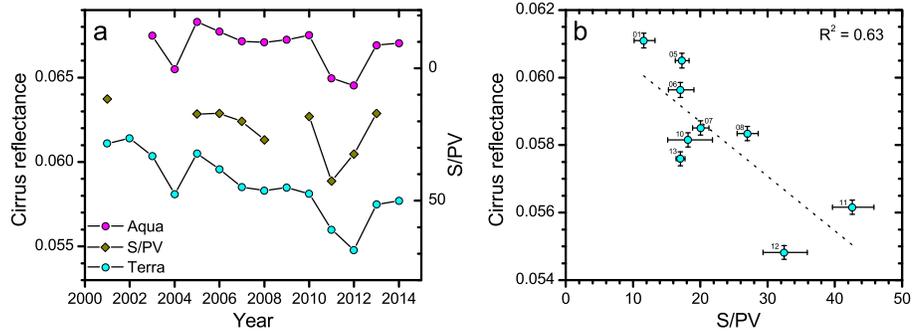
4.2.1. Comparison to the MODIS Retrieved Cirrus Reflectance
To explore a possible impact of downwelling stratospheric aerosol on cirrus clouds, the particulate sulfur concentration measured during CARIBIC is compared to the CR retrieved by MODIS (see section 2.7). Because of the scarcity of UT data we use the S/PV in the LMS as a reasonable proxy for the UT particulate sulfur, as validated above (using samples collected below 5 PVU as in Figure 6). Only the season with

Figure 7. (a) Time series of the geometric average S/PV in the LMS (S/PV$_{LMS}$; ng m^{-3} STP/PVU) (note the reversed scale) and the arithmetic average of the MODIS-retrieved parameter, cirrus reflectance (CR) from Aqua and Terra, for samples taken below 5 PVU in the season March–July. (b) A comparison of S/PV and Terra's CR as in Figure 7a. A linear regression fit is shown as a dotted line.

largest stratospheric impact on the UT/LMS (March–July) is investigated here. The comparison is illustrated as time series (Figure 7a) of each year's average S/PV from CARIBIC and CR from the Terra and Aqua satellites. While no CARIBIC measurements were performed in the years 2003 and 2004, also the years 2002 and 2009 need to be excluded since too few months of CARIBIC data are available for these years.

The year-to-year changes of the CR of both satellites agree very well, in which the average Aqua values are ~20% higher, see explanation in section 2.7. The year-to-year variability and the general trend in S/PV are anticorrelated to CR; note the inverted scale of S/PV (Figure 7a). S/PV increases gradually from 2001 until 2011/2012 as a result of volcanism, whereas CR decreases. The increase in CR after the year 2012 coincides with less volcanic aerosol in the LMS. Unfortunately, maintenance of the CARIBIC aircraft in the year 2014 resulted in too few measurement months to include that year in the comparison, but the volcanic activity is known to have been low. The rate of CR decrease of Aqua is slightly weaker than that of Terra, which could be caused by stronger influence of convection. Since the CR obtained by Terra is less influenced by convective activity, it is expected to be more sensitive to changes in the UT/LMS conditions, which in this case concerns changes in the sulfur concentrations. We therefore use the CR of Terra to illustrate the close coupling of S/PV and CR as a scatterplot (Figure 7b). A linear regression reveals a good anticorrelation between CR and S/PV ($R^2 = 0.63$) with a significance level of 99%, even though the two parameters compared were obtained using fundamentally different measurement methods (the corresponding results for Aqua are $R^2 = 0.74$, significance level of 99%). The relative decrease in CR between 2001 and 2011 is 8 ± 2%, while the particulate sulfur concentration in LMS increased by a factor of 3–4 during this time.

In Figure 8, the average CR during 2 years of low volcanic influence (2001–2002) is compared to the average CR during the 2 years of highest volcanic influence on the LMS/UT (2011–2012). The observed CR is generally higher over areas where convection is common since this gives rise to anvils (Figures 8a and 8b). This can be seen in the eastern parts of the oceans where warm water is transported northward resulting in convection and over the North American continent where convection also is common during this season. The CR decreases from 2001–2002 to 2011–2012 for large parts of the NH midlatitudes, see Figure 8c, and the largest decreases are found over Europe, the Atlantic Ocean, the North American continent, and the mid-Pacific Ocean. Change in the location or decrease in convective activity over the eastern parts of the oceans or the North American continent may cause a change in the CR (Figure 8c). However, limiting the computations to areas without persistent convection slightly increased the correlation between the Terra CR and S/PV. Hence, the anticorrelation seen in Figure 7b cannot be explained by a change in convective activity. In the following section possible causes for the anticorrelation will be discussed.

4.2.2. Cloud Microphysics and Climate

Recent geoengineering (GE) studies suggest that increased stratospheric sulfurous aerosol concentration can decrease cirrus cloud reflectance in a homogeneous nucleation regime. The GE aerosol increases temperatures and decreases vertical velocities in the tropopause region, which reduce the ice crystal formation rate, leading to optically thinner clouds [*Kuebbeler et al.*, 2012].
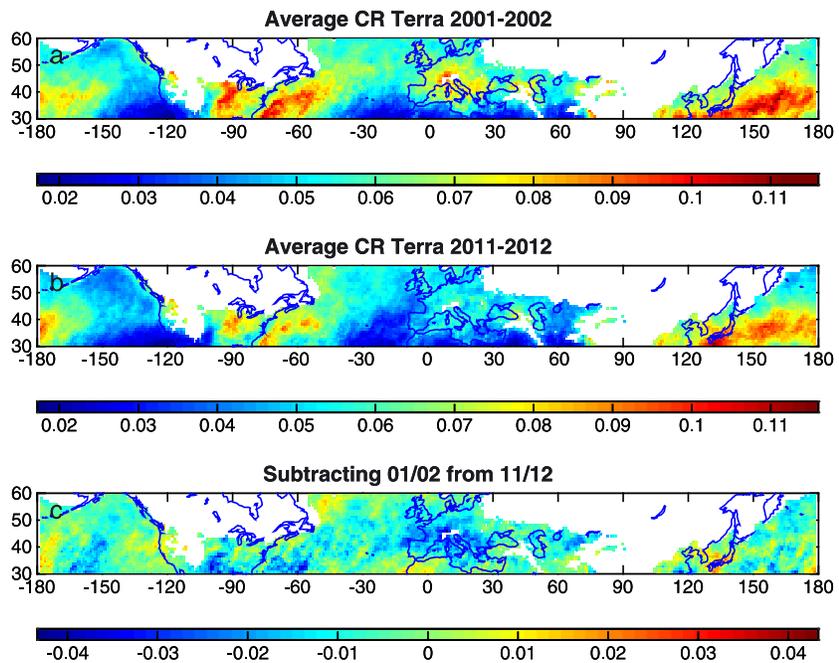
Figure 8. Geographical distributions of the March–July CR averaged over the years of (a) background concentrations of sulfur (2001–2002), (b) years of strongest influence of volcanism (2011–2012), and (c) the difference in CR between the years in Figures 8b and 8a.

Sulfurous aerosol could also shift the freezing mechanism of the cirrus clouds from homogeneous to heterogeneous. If the sulfuric acid is neutralized by ammonia, the downwelling LMS aerosol could act as IN [*Abbatt et al.*, 2006; *Hoose and Möhler*, 2012]. Increases in IN concentrations could shift the freezing mechanism from homogenous to heterogeneous, creating optically thinner cirrus clouds with fewer, larger ice crystals. Seeding of cirrus clouds have been found to make them optically thinner, except in pure heterogeneous freezing regimes [*Storelvmo and Herger*, 2014].

In a heterogeneous nucleation regime, a decrease in the amount of IN would reduce the number of ice crystals in the cirrus clouds, making them optically thinner. Sulfuric acid aerosol downwelling from the LMS may interact with some of the IN present in the UT, reducing their nucleation abilities and that way decrease the number of IN. Deactivation of soot IN from aviation could provide an explanation to the pronounced CR decrease over the Atlantic, North America, and Europe, as a large fraction of the soot emitted from the aviation corridor over the northern Atlantic ends up in this region [*Zhou and Penner*, 2014].

One of the discussed mechanisms, or a combination of them, may have caused the decrease in CR seen in Figures 7 and 8. A decrease in CR implies that the clouds are optically thinner and both reflect less shortwave radiation and absorb less longwave radiation. Because the latter effect dominates, a decrease in CR corresponds to a smaller greenhouse effect from cirrus clouds [*Storelvmo et al.*, 2013].

The strong response of 8% decrease in CR to a 3.5-fold increase of S/PV in the LMS indicates a substantial radiative forcing. Making use of the fact that CR and cloud optical thickness (COT) are linearly dependent for thin clouds [*Meyer et al.*, 2007], and the sensitivity of net radiative forcing to changes in COT according to *Cirisan et al.* [2013, their Figure 8] the maximum decrease of 8% of CR in the time period studied corresponds to approximately $-2\,Wm^{-2}$ in net radiative forcing at NH midlatitudes. This regional result pertains to the season March to July.

5. Conclusions

This study focuses on particulate sulfur in the Northern Hemisphere's upper troposphere (UT) and lowermost stratosphere (LMS) in the period 1999–2013 measured by the CARIBIC observatory. Particulate sulfur

concentrations varied by a factor of about 100 in this period, mainly as a result of volcanic injections. The sulfurous aerosol concentration in the UT was strongly connected to that in the LMS, as downwelling aerosol constituted the major fraction of the UT particulate sulfur concentration in the periods of volcanic influence.

During the 15 year time span, the UT/LMS was perturbed by volcanism to various degrees. The lowest sulfur concentrations were observed in 1999–2002, a volcanically quiescent period. The largest perturbations were found not only after extratropical volcanic eruptions, specifically in 2008 (Kasatochi) and 2009 (Sarychev), but also in fall 2011 to spring 2012 after an eruption of the tropical volcano Nabro.

In the periods 2005–2008 and 2013, the variability in sulfur concentration was dominated by downwelling of volcanic aerosol from tropical volcanism that was transported through the stratosphere. In that period, the LMS sulfur concentration peaked in May as a result of downwelling of air transported in the deep Brewer-Dobson branch. The same seasonal variation was found in the UT, illustrating a strong coupling of the LMS and the UT. Downwelling of volcanic aerosol was found to more than double the spring and summer UT particulate sulfur concentrations compared to the background levels.

A comparison of sulfur concentrations to satellite observations of the MODIS retrieved cirrus reflectance (CR) from the satellites Terra and Aqua, for the season of largest stratospheric impact on the UT and LMS (March–July), resulted in strong anticorrelations ($R^2 = 0.63$ (Terra), $R^2 = 0.72$ (Aqua). The CR and thereby the cloud optical thickness (COT) decreased by 8% in the period 2001–2011. During this time the particulate sulfur concentration increased by a factor of 3.5 in the LMS. The strongest reduction in CR occurs over North America, the North Atlantic, and Europe, where soot ice nuclei (IN) from aviation [*Schumann et al.*, 2013] could shift the cirrus freezing mechanism from homogeneous to heterogeneous [*Zhou and Penner*, 2014], making deactivation of IN by volcanic sulfate aerosol a conceivable explanation for the observed reduction in CR. However, more research is needed to establish the definite mechanism.

Previous studies have shown that volcanism induced a significant radiative forcing after the turn of the millennium [*Santer et al.*, 2014; *Solomon et al.*, 2011] by the direct effect from stratospheric aerosol. New findings of the importance of LMS aerosol in this respect further increase this estimated forcing [*Andersson et al.*, 2015; *Ridley et al.*, 2014]. The tropical Pacific cooling [*England et al.*, 2014; *Meehl and Teng*, 2014], variations in solar forcing [*Flato et al.*, 2013], and volcanic aerosol forcing occurring after the year 2000 [*Santer et al.*, 2014; *Solomon et al.*, 2011] are not captured by the CMIP5 (Coupled Model Intercomparison Project Phase 5) models used by the Intergovernmental Panel on Climate Change, resulting in overestimation of the global warming over the last 15 years [*Flato et al.*, 2013; *Fyfe et al.*, 2013]. Here we introduce an indirect effect from volcanic aerosol that can contribute further explanation of the mismatch of model results and observations.

References

Abbatt, J. P. D., S. Benz, D. J. Cziczo, Z. Kanji, U. Lohmann, and O. Mohler (2006), Solid ammonium sulfate aerosols as ice nuclei: A pathway for cirrus cloud formation, *Science*, *313*(5794), 1770–1773.

Agrawal, H., A. A. Sawant, K. Jansen, J. W. Miller, and D. R. Cocker III (2008), Characterization of chemical and particulate emissions from aircraft engines, *Atmos. Environ.*, *42*, 4380–4392.

Andersson, S. M., B. G. Martinsson, J. Friberg, C. A. M. Brenninkmeijer, A. Rauthe-Schöch, M. Hermann, P. F. J. van Velthoven, and A. Zahn (2013), Composition and evolution of volcanic aerosol from eruptions of Kasatochi, Sarychev and Eyjafjallajökull in 2008–2010 based on CARIBIC observations, *Atmos. Chem. Phys.*, *13*, doi:10.5194/acp-13-1781-2013.

Andersson, S. M., B. G. Martinsson, J.-P. Vernier, J. Friberg, C. A. M. Brenninkmeijer, M. Hermann, P. F. J. van Velthoven, and A. Zahn (2015), Significant radiative impact of volcanic aerosol in the lowermost stratosphere, *Nat. Commun.*, *6*, doi:10.1038/ncomms8692.

Barahona, D., A. Molod, J. Bacmeister, A. Nenes, A. Gettelman, H. Morrison, V. Phillips, and A. Eichmann (2014), Development of two-moment cloud microphysics for liquid and ice within the NASA Goddard Earth Observing System Model (GEOS-5), *Geosci. Model Dev.*, *7*(4), doi:10.5194/gmd-7-1733-2014.

Baran, A. J. (2009), A review of the light scattering properties of cirrus, *J. Quant. Spectros. Radiat. Transfer*, *110*(14), doi:10.1016/j.jqsrt.2009.02.026.

Bönisch, H., A. Engel, J. Curtius, T. Birner, and P. Hoor (2009), Quantifying transport into the lowermost stratosphere using simultaneous in-situ measurements of SF6 and CO₂, *Atmos. Chem. Phys.*, *9*, 5905–5919.

Boucher, O., et al. (2013), Clouds and aerosols, in *Climate Change 2013: The Physical Science Basis. Contribution of Working Group I to the Fifth Assessment Report of the Intergovernmental Panel on Climate Change*, Cambridge Univ. Press, Cambridge, U. K., and New York.

Bourassa, A. E., A. Robock, W. J. Randel, T. Deshler, L. A. Rieger, N. D. Lloyd, E. J. T. Llewellyn, and D. A. Degenstein (2012), Large volcanic aerosol load in the stratosphere linked to Asian monsoon transport, *Science*, *337*(6090), doi:10.1126/science.1219371.

Brenninkmeijer, C. A. M., P. J. Crutzen, H. Fischer, W. Güsten, W. Hans, G. Heinrich, J. Heintzenberg, M. Hermann, T. Immelmann, and D. Kersting (1999), CARIBIC-Civil aircraft for global measurement of trace gases and aerosols in the tropopause region, *J. Atmos. Oceanic Technol.*, *16*(10), 1373–1383.

Brenninkmeijer, C. A. M., et al. (2007), Civil aircraft for the regular investigation of the atmosphere based on an instrumented container: The new CARIBIC system, *Atmos. Chem. Phys.*, *7*(18), 4953–4976.

Campbell, J. R., E. J. Welton, N. A. Krotkov, K. Yang, S. A. Stewart, and M. D. Fromm (2012), Likely seeding of cirrus clouds by stratospheric Kasatochi volcanic aerosol particles near a mid-latitude tropopause fold, *Atmos. Environ.*, *46*, doi:10.1016/j.atmosenv.2011.09.027.

Carn, S. A., and F. J. Prata (2010), Satellite-based constraints on explosive SO2 release from Soufrière Hills Volcano, Montserrat, *Geophys. Res. Lett.*, *37*, L00E22, doi:10.1029/2010GL044971.

Carn, S. A., A. J. Krueger, N. A. Krotkov, K. Yang, and K. Evans (2009), Tracking volcanic sulfur dioxide clouds for aviation hazard mitigation, *Nat. Hazards*, *51*(2), doi:10.1007/s11069-008-9228-4.

Chen, T., W. B. Rossow, and Y. Zhang (2000), Radiative effects of cloud-type variations, *J. Clim.*, *13*(1), 264–286.

Cirisan, A., P. Spichtinger, B. P. Luo, D. K. Weisenstein, H. Wernli, U. Lohmann, and T. Peter (2013), Microphysical and radiative changes in cirrus clouds by geoengineering the stratosphere, *J. Geophys. Res. Atmos.*, *118*, 4533–4548, doi:10.1002/jgrd.50388.

Clarisse, L., D. Hurtmans, C. Clerbaux, J. Hadji-Lazaro, Y. Ngadi, and P.-F. Coheur (2012), Retrieval of sulphur dioxide from the infrared atmospheric sounding interferometer (IASI), *Atmos. Meas. Tech.*, *5*(3), doi:10.5194/amt-5-581-2012.

Crutzen, P. J. (1976), The possible importance of CSO for the sulfate layer of the stratosphere, *Geophys. Res. Lett.*, *3*(2), 73–76, doi:10.1029/GL003i002p00073.

Cziczo, D. J., K. D. Froyd, C. Hoose, E. J. Jensen, M. Diao, M. A. Zondlo, J. B. Smith, C. H. Twohy, and D. M. Murphy (2013), Clarifying the dominant sources and mechanisms of cirrus cloud formation, *Science*, *340*(6138), doi:10.1126/science.1234145.

DeMott, P. J., D. J. Cziczo, A. J. Prenni, D. M. Murphy, S. M. Kreidenweis, D. S. Thomson, R. Borys, and D. C. Rogers (2003), Measurements of the concentration and composition of nuclei for cirrus formation, *Proc. Natl. Acad. Sci. U.S.A.*, *100*(25), 14,655–14,660.

Deshler, T. (2008), A review of global stratospheric aerosol: Measurements, importance, life cycle, and local stratospheric aerosol, *Atmos. Res.*, *90*(2), 223–232.

England, M. H., S. McGregor, P. Spence, G. A. Meehl, A. Timmermann, W. Cai, A. S. Gupta, M. J. McPhaden, A. Purich, and A. Santoso (2014), Recent intensification of wind-driven circulation in the Pacific and the ongoing warming hiatus, *Nat. Clim. Change*, *4*(3), 222–227.

Flato, G., J. Marotzke, B. Abiodun, P. Braconnot, S. Chou, W. Collins, P. Cox, F. Driouech, S. Emori, and V. Eyring (2013), Evaluation of climate models, in *Climate Change 2013: The Physical Science Basis. Contribution of Working Group I to the Fifth Assessment Report of the Intergovernmental Panel on Climate Change*, pp. 741–866, Cambridge Univ. Press, Cambridge.

Friberg, J., B. G. Martinsson, S. M. Andersson, C. A. M. Brenninkmeijer, M. Hermann, P. F. J. van Velthoven, and A. Zahn (2014), Sources of increase in lowermost stratospheric sulphurous and carbonaceous aerosol background concentrations during 1999–2008 derived from CARIBIC flights, *Tellus B*, *66*.

Fusina, F., P. Spichtinger, and U. Lohmann (2007), Impact of ice supersaturated regions and thin cirrus on radiation in the midlatitudes, *J. Geophys. Res.*, *112*, D24S14, doi:10.1029/2007JD008449.

Fyfe, J. C., N. P. Gillett, and F. W. Zwiers (2013), Overestimated global warming over the past 20 years, *Nat. Clim. Change*, *3*(9), 767–769.

Gao, B.-C., and Y. J. Kaufman (1995), Selection of the 1.375-um MODIS channel for remote sensing of cirrus clouds and stratospheric aerosols from space, *J. Atmos. Sci.*, *52*(23), 4231–4237.

Gao, B.-C., P. Yang, W. Han, R.-R. Li, and W. J. Wiscombe (2002), An algorithm using visible and 1.38-μm channels to retrieve cirrus cloud reflectances from aircraft and satellite data, *Geosci. Remote Sens., IEEE Trans.*, *40*(8), 1659–1668.

Gettelman, A., and C. Chen (2013), The climate impact of aviation aerosols, *Geophys. Res. Lett.*, *40*, 2785–2789, doi:10.1002/grl.50520.

Guan, H., R. Esswein, J. Lopez, R. Bergstrom, A. Warnock, M. Follette-Cook, M. Fromm, and L. T. Iraci (2010), A multi-decadal history of biomass burning plume heights identified using aerosol index measurements, *Atmos. Chem. Phys.*, *10*, doi:10.5194/acp-10-6461-2010.

GVP (2011), Global Volcanism Program. [Availble at http://www.volcano.si.edu/index.cfm, 15 March 2012.]

Haywood, J. M., A. Jones, L. Clarisse, A. Bourassa, J. Barnes, P. Telford, N. Bellouin, O. Boucher, P. Agnew, and C. Clerbaux (2010), Observations of the eruption of the Sarychev volcano and simulations using the HadGEM2 climate model, *J. Geophys. Res.*, *115*, D21212, doi:10.1029/2010JD014447.

Hermann, M., F. Stratmann, M. Wilck, and A. Wiedensohler (2001), Sampling characteristics of an aircraft-borne aerosol inlet system, *J. Atmos. Oceanic Technol.*, *18*(1), 7–19.

Hoerling, M. P., T. K. Schaack, and A. J. Lenzen (1991), Global objective tropopause analysis, *Mon. Weather Rev.*, *119*, 1816–1831.

Hofmann, D., J. Barnes, M. O'Neill, M. Trudeau, and R. Neely (2009), Increase in background stratospheric aerosol observed with lidar at Mauna Loa Observatory and Boulder, Colorado, *Geophys. Res. Lett.*, *36*, L15808, doi:10.1029/2009GL039008.

Hoinka, K. P. (1997), The tropopause: Discovery, definition and demarcation, *Meteorol. Z.*, *6*, 281–303.

Holton, J. R., P. H. Haynes, M. E. McIntyre, A. R. Douglas, R. B. Rood, and L. Pfister (1995), Stratosphere-troposphere exchange, *Rev. Geophys.*, *33*(4), 403–439, doi:10.1029/95RG02097.

Hoor, P., C. Gurk, D. Brunner, M. I. Hegglin, H. Wernli, and H. Fischer (2004), Seasonality and extent of extratropical TST derived from in-situ CO measurements during SPURT, *Atmos. Chem. Phys.*, *4*(5), 1427–1442.

Hoose, C., and O. Möhler (2012), Heterogeneous ice nucleation on atmospheric aerosols: A review of results from laboratory experiments, *Atmos. Chem. Phys.*, *12*(20), doi:10.5194/acp-12-9817-2012.

Jensen, E. J., L. Pfister, T. P. Bui, P. Lawson, and D. Baumgardner (2010), Ice nucleation and cloud microphysical properties in tropical tropopause layer cirrus, *Atmos. Chem. Phys.*, *10*(3), 1369–1384.

Johansson, S. A. E., and J. L. Campbell (1988), *PIXE: A Novel Technique for Elemental Analysis*, 347 pp., John Wiley, Hoboken, N. J.

Karcher, B., and U. Lohmann (2002), A parameterization of cirrus cloud formation: Homogeneous freezing including effects of aerosol size, *J. Geophys. Res.*, *107*(D23), 4698, doi:10.1029/2001JD001429.

Kuebbeler, M., U. Lohmann, and J. Feichter (2012), Effects of stratospheric sulfate aerosol geo-engineering on cirrus clouds, *Geophys. Res. Lett.*, *39*, L23803, doi:10.1029/2012GL053797.

Kuebbeler, M., U. Lohmann, J. Hendricks, and B. Karcher (2014), Dust ice nuclei effects on cirrus clouds, *Atmos. Chem. Phys.*, *14*(6), 3027–3046.

Lohmann, U., B. Karcher, and C. Timmreck (2003), Impact of the Mount Pinatubo eruption on cirrus clouds formed by homogeneous freezing in the ECHAM4 GCM, *J. Geophys. Res.*, *108*(D18), 4568, doi:10.1029/2002JD003185.

Lopez, T. M., S. A. Carn, P. Webley, M. A. Pfeffer, M. P. Doukas, P. J. Kelly, C. A. Werner, F. Prata, D. J. Schneider, and C. F. Cahill (2009), Evaluation of satellite derived sulfur dioxide measurements for volcano monitoring during the 2009 Redoubt eruption, *AGU, Fall Meeting 2009*, abstract #V51F-03.

Luo, Z. Z., W. B. Rossow, T. Inoue, and C. J. Stubenrauch (2002), Did the eruption of the Mt. Pinatubo Volcano affect cirrus properties?, *J. Clim.*, *15*(19), 2806–2820.

Martinsson, B. G., H. N. Nguyen, C. A. M. Brenninkmeijer, A. Zahn, J. Heintzenberg, M. Hermann, and P. F. J. van Velthoven (2005), Characteristics and origin of lowermost stratospheric aerosol at northern midlatitudes under volcanically quiescent conditions based on CARIBIC observations, *J. Geophys. Res.*, *110*, D12201, doi:10.1029/2004JD005644.

Martinsson, B. G., C. A. M. Brenninkmeijer, S. A. Carn, M. Hermann, K. P. Heue, P. F. J. van Velthoven, and A. Zahn (2009), Influence of the 2008 Kasatochi volcanic eruption on sulfurous and carbonaceous aerosol constituents in the lower stratosphere, *Geophys. Res. Lett.*, *36*, L12813, doi:10.1029/2009GL038735.

Martinsson, B. G., J. Friberg, S. M. Andersson, A. Weigelt, M. Hermann, D. Assmann, J. Voigtländer, C. A. M. Brenninkmeijer, P. J. F. van Velthoven, and A. Zahn (2014), Comparison between CARIBIC aerosol samples analysed by accelerator-based methods and optical particle counter measurements, *Atmos. Meas. Tech.*, *7*, doi:10.5194/amt-7-2581-2014.

Meehl, G. A., and H. Teng (2014), CMIP5 multi-model hindcasts for the mid-1970s shift and early 2000s hiatus and predictions for 2016–2035, *Geophys. Res. Lett.*, *41*, 1711–1716, doi:10.1002/2014GL059256.

Meyer, K., and S. Platnick (2010), Utilizing the MODIS 1.38 μm channel for cirrus cloud optical thickness retrievals: Algorithm and retrieval uncertainties, *J. Geophys. Res.*, *115*, D24209, doi:10.1029/2010JD014872.

Meyer, K., P. Yang, and B.-C. Gao (2007), Ice cloud optical depth from MODIS cirrus reflectance, *IEEE Geosci. Rem. Sens. Lett.*, *4*(3), 471–474.

Mitchell, D. L., R. P. Lawson, and S. Mishra (2011), *Cirrus Clouds and Climate Engineering: New Findings on Ice Nucleation and Theoretical Basis*, INTECH Open Access Publisher.

Murphy, D. M., D. S. Thomson, and M. J. Mahoney (1998), In situ measurements of organics, meteoritic material, mercury, and other elements in aerosols at 5 to 19 kilometers, *Science*, *282*(5394), 1664–1669.

Murphy, D. M., D. J. Cziczo, K. D. Froyd, P. K. Hudson, B. M. Matthew, A. M. Middlebrook, R. E. Peltier, A. Sullivan, D. S. Thomson, and R. J. Weber (2006), Single-particle mass spectrometry of tropospheric aerosol particles, *J. Geophys. Res.*, *111*, D23S32, doi:10.1029/2006JD007340.

Murphy, D. M., K. D. Froyd, J. P. Schwarz, and J. C. Wilson (2014), Observations of the chemical composition of stratospheric aerosol particles, *Q. J. R. Meteorol. Soc.*, *140*, 1269–1278.

Myhre, G., D. Shindell, F. Bréon, W. Collins, J. Fuglestvedt, J. Huang, D. Koch, J. Lamarque, D. Lee, and B. Mendoza (2013), Anthropogenic and natural radiative forcing, in *Climate Change 2013: The Physical Science Basis. Contribution of Working Group I to the Fifth Assessment Report of the Intergovernmental Panel on Climate Change*, edited by T. F. Stocker et al., Cambridge Univ. Press, Cambridge, U. K., and New York.

Nguyen, H. N., A. Gudmundsson, and B. G. Martinsson (2006), Design and calibration of a multi-channel aerosol sampler for tropopause region studies from the CARIBIC platform, *Aerosol Sci. Technol.*, *40*, doi:10.1080/02786820600767807.

Nguyen, H. N., et al. (2008), Chemical composition and morphology of individual aerosol particles from a CARIBIC flight at 10 km altitude between 50°N and 30°S, *J. Geophys. Res.*, *113*, D23209, doi:10.1029/2008JD009956.

Pan, L. L., W. J. Randel, B. L. Gary, M. J. Mahoney, and E. J. Hintsa (2004), Definitions and sharpness of the extratropical tropopause: A trace gas perspective, *J. Geophys. Res.*, *109*, D23103, doi:10.1029/2004JD004982.

Papaspiropoulos, G., B. Mentes, P. Kristiansson, and B. G. Martinsson (1999), A high sensitivity elemental analysis methodology for upper tropospheric aerosol, *Nucl. Instrum. Methods Phys. Res., Sect. B*, *150*, 356–362.

Platnick, S., M. D. King, S. A. Ackerman, W. P. Menzel, B. A. Baum, J. C. Riedi, and R. A. Frey (2003), The MODIS cloud products: Algorithms and examples from Terra, *IEEE Trans. Geosci. Remote*, *41*(2), 459–473.

Prata, A. J., and C. Bernardo (2007), Retrieval of volcanic SO_2 column abundance from atmospheric infrared sounder data, *J. Geophys. Res.*, *112*, D20204, doi:10.1029/2006JD007955.

Pruppacher, H. R., and J. D. Klett (1997), *Microphysics of Clouds and Precipitation*, Kluwer Acad., Dordrecht, Netherlands.

Rauthe-Schöch, A., et al. (2012), CARIBIC aircraft measurements of Eyjafjallajökull volcanic clouds in April/May 2010, *Atmos. Chem. Phys.*, *12*, doi:10.5194/acp-12-879-2012.

Reid, J. S., R. Koppmann, T. F. Eck, and D. P. Eleuterio (2005), A review of biomass burning emissions Part II: Intensive physical properties of biomass burning particles, *Atmos. Chem. Phys.*, *5*(3), 799–825.

Ridley, D. A., S. Solomon, J. E. Barnes, V. D. Burlakov, T. Deshler, S. I. Dolgii, A. B. Herber, T. Nagai, R. R. Neely, and A. V. Nevzorov (2014), Total volcanic stratospheric aerosol optical depths and implications for global climate change, *Geophys. Res. Lett.*, *41*, 7763–7769, doi:10.1002/2014GL061541.

Robock, A. (2000), Volcanic eruptions and climate, *Rev. Geophys.*, *38*(2), 191–219, doi:10.1029/1998RG000054.

Rosen, J. M. (1971), The boiling point of stratospheric aerosols, *J. Appl. Meteorol.*, *10*, 1044–1046.

Santer, B. D., C. Bonfils, J. F. Painter, M. D. Zelinka, C. Mears, S. Solomon, G. A. Schmidt, J. C. Fyfe, J. N. S. Cole, and L. Nazarenko (2014), Volcanic contribution to decadal changes in tropospheric temperature, *Nat. Geosci.*, *7*(3), 185–189.

Schmale, J., et al. (2010), Aerosol layers from the 2008 eruptions of Mount Okmok and Mount Kasatochi: In situ upper troposphere and lower stratosphere measurements of sulfate and organics over Europe, *J. Geophys. Res.*, *115*, D00L07, doi:10.1029/2009JD013628.

Schumann, U., P. Jeßberger, and C. Voigt (2013), Contrail ice particles in aircraft wakes and their climatic importance, *Geophys. Res. Lett.*, *40*, 2867–2872, doi:10.1002/grl.50539.

Solomon, S., J. S. Daniel, R. R. Neely, J. P. Vernier, E. G. Dutton, and L. W. Thomason (2011), The persistently variable "background" stratospheric aerosol layer and global climate change, *Science*, *333*, doi:10.1126/science.1206027.

Song, N. H., D. O. Starr, D. J. Wuebbles, A. Williams, and S. M. Larson (1996), Volcanic aerosols and interannual variation of high clouds, *Geophys. Res. Lett.*, *23*(19), 2657–2660, doi:10.1029/96GL02372.

Sprenger, M., and H. Wernli (2003), A northern hemispheric climatology of cross-tropopause exchange for the ERA15 time period (1979–1993), *J. Geophys. Res.*, *108*(D12), 8521, doi:10.1029/2002JD002636.

Storelvmo, T., and N. Herger (2014), Cirrus cloud susceptibility to the injection of ice nuclei in the upper troposphere, *J. Geophys. Res. Atmos.*, *119*, 2375–2389.

Storelvmo, T., J. E. Kristjansson, H. Muri, M. Pfeffer, D. Barahona, and A. Nenes (2013), Cirrus cloud seeding has potential to cool climate, *Geophys. Res. Lett.*, *40*, 178–182, doi:10.1029/2012GL054201.

Thomas, H. E., I. M. Watson, S. A. Carn, A. J. Prata, and V. J. Realmuto (2011), A comparison of AIRS, MODIS and OMI sulphur dioxide retrievals in volcanic clouds, *Geomat. Nat. Hazard. Risk*, *2*(3), doi:10.1080/19475705.2011.564212.

Vernier, J. P., et al. (2011), Major influence of tropical volcanic eruptions on the stratospheric aerosol layer during the last decade, *Geophys. Res. Lett.*, *38*, L12807, doi:10.1029/2011GL047563.

Weisenstein, D. K., G. K. Yue, M. K. W. Ko, N. D. Sze, J. M. Rodriguez, and C. J. Scott (1997), A two-dimensional model of sulfur species and aerosols, *J. Geophys. Res.*, *102*(D11), 13,019–13,035, doi:10.1029/97JD00901.

Wylie, D. P., and W. P. Menzel (1999), Eight years of high cloud statistics using HIRS, *J. Clim.*, *12*(1), 170–184.

Yang, K., X. Liu, P. K. Bhartia, N. A. Krotkov, S. A. Carn, E. J. Hughes, A. J. Krueger, R. J. D. Spurr, and S. G. Trahan (2010), Direct retrieval of sulfur dioxide amount and altitude from spaceborne hyperspectral UV measurements: Theory and application, *J. Geophys. Res.*, *115*, D00L09, doi:10.1029/2010JD013982.

Zahn, A., and C. A. M. Brenninkmeijer (2003), New directions: A chemical tropopause defined, *Atmos. Environ.*, *37*(3), 439–440.

Zahn, A., E. Christner, P. F. J. Velthoven, A. Rauthe-Schöch, and C. A. M. Brenninkmeijer (2014), Processes controlling water vapor in the upper troposphere/lowermost stratosphere: An analysis of 8 years of monthly measurements by the IAGOS-CARIBIC observatory, *J. Geophys. Res. Atmos.*, *119*, 11,505–11,525, doi:10.1002/2014JD021687.

Zhou, C., and J. E. Penner (2014), Aircraft soot indirect effect on large-scale cirrus clouds: Is the indirect forcing by aircraft soot positive or negative?, *J. Geophys. Res. Atmos.*, *119*, 11,303–11,320.